Surface structure of domain walls

1998 J. Phys.: Condens. Matter 10 L359

(http://iopscience.iop.org/0953-8984/10/21/005)

J. Phys.: Condens. Matter **10** (1998) L359–L366. Printed in the UK PII: S0953-8984(98)92611-X

LETTER TO THE EDITOR

Surface structure of domain walls

Jurica Novak and Ekhard K H Salje

Department of Earth Sciences, University of Cambridge, Downing Street, Cambridge CB2 3EQ, UK

Received 18 March 1998

Abstract. The results of a numerical simulation of the surface structure of an orthogonally intersecting twin domain wall in a ferroelastic lattice are presented. The twin wall is seen at the surface as a pitched roof structure. The centre of the wall appears as a rounding of the ridge. The thickness of the ridge is the same as the thickness of the twin domain wall in the bulk. In contrast to this simple shape of the relaxed surface, the elastic response is rather exotic. We predict that AFM images taken in tapping mode should show a narrow groove at the middle of the ridge with two hill-like features on either side of the groove. Consequences for the chemical activity of the sites close to the ridge are discussed.

Domain patterns are often a desirable characteristic of device materials, notably in ferroelectrics and ferroelastics. The elementary process for the pattern formation is, in many cases, ferroelastic twinning [1]. Typical examples for twin related patterns are high-T_c superconductors, relaxor materials, perovskite substrates, palmierites, leucites, quartz and feldspars [1]. Pattern formation can be spontaneous, as well as induced by some external field exerted on a sample or a device material [1].

Walls between two twin-related domains are areas of high chemical reactivity [2], fast diffusion and electronic properties which can be quite different from those of the bulk material. With respect to many physical and chemical properties, twin walls behave like grain boundaries, with the advantage that twin walls can be tailored easily [1], especially if of ferroelastic origin. The main disadvantage of twin walls is that they are difficult to investigate, despite the fact that they appear as distinctive features in transition electron microscopical (TEM) images [3]. Any fine structures may be significantly changed when samples are prepared as atomically thin slabs or wedges for TEM studies which makes their study virtually impossible. A more subtle mode of investigation uses x-ray diffraction, although this technique does not yet allow the analysis of the chemically important intersection of a twin wall with the surface of a sample [4]. The third mode of investigation is by atomic force microscopy or related techniques which are sensitive to spatial variation in surface topography or physical properties of material [5, 6, 7, 8]. These latter techniques have, despite several attempts, failed to precisely determine any fine structure of the twin walls close to surfaces.

Analytically, the ferroelastic materials have been well described using the Landau–Ginzburg phenomenological model, which expresses the Gibbs free energy as a polynomial in the order parameter and its spatial derivative [1]. This method, though, has not been employed to deal with the details of the surface properties of domain walls. The wall profile at the surface is in fact a double relaxational problem, including both the surface and the domain wall relaxation. Each of these problems has been successfully solved using the Landau–Ginzburg model, but only when approached separately. The complexity of

the problem arises from the inherent multi-dimensionality when surface and domain wall relaxations are considered concurrently [9].

In this letter we show that a numerical simulation of a two-dimensional twinning lattice provides a clear and precise insight into the structure of a twin domain wall near and at the surface.

The imaging techniques predominant in the study of surface properties of domain walls do not generally image the real space topography of the surface [6]. Here we show that there are two features that can be identified as fingerprints of a twin domain wall at the surface. In real space, the fingerprint is a rounded wedge. The other, more interesting, fingerprint is a groove, with a ridge on both sides, obtained as an elastic response to a force normal to the surface.

The model we use to simulate twin domains and the wall between them is a simple two-dimensional lattice that represents a hypothetical plane perpendicular to a twin wall in the ferroelastic phase. The twin domains are generated by the elastic shear deformation of the square unit cells. Such deformation (i.e. spontaneous strain in a ferroelastic material) is rather general as discussed above, and is always the reason for ferroelastic twinning [1]. In our generic model [10, 11] we represent atoms as points interacting via elastic potentials.

Each point at the site (i, j) has two degrees of freedom, the two coordinates $X_{i,j}$ and $Y_{i,j}$. In order to generate surface relaxations it is essential that interatomic interactions extend to, at least, two interatomic layers perpendicular to the surface [12]. Therefore, each lattice point (i, j) interacts explicitly with the points populating its third and lower coordination shells, and interactions for larger distances are truncated. To successfully describe the structure of a domain wall at the surface, we needed to simulate only two free surfaces, those perpendicular to the wall itself. This approach yields three distinctive classes of points in the model, those in the bulk, interacting with twelve neighbours, then those in the layer next to the surface, interacting with eleven neighbours, and finally, the points in the surface layer having only eight neighbours to interact with. Lennard-Jones potentials are used for second- and third-nearest-neighbour interactions, and harmonic potentials are used for nearest neighbour interactions. We used a harmonic potential in order to preserve the lattice configuration, effectively keeping the lattice parameter at a constant value throughout the simulation. The potential energy of a point (i, j) can be written as:

$$\mathcal{U}_p(i, j) = \sum_{n=1}^{p} \mathcal{U}_n(|\boldsymbol{r}|) \tag{1}$$

where the subscript p denotes the position of the point and the number of neighbours it interacts with:

$$p = \begin{cases} 12 & \text{bulk} \\ 11 & \text{next to surface} \\ 8 & \text{surface} \end{cases}$$

and $\mathcal{U}_n(|\boldsymbol{r}|)$ is:

$$\mathcal{U}_n(|\boldsymbol{r}|) = \begin{cases} \frac{1}{2}\,\kappa\,(|\boldsymbol{r}| - a)^2 & \text{nearest neighbours} \\ \varepsilon^* \left[\frac{r^{*12}}{|\boldsymbol{r}|^{12}} - 2\frac{r^{*6}}{|\boldsymbol{r}|^6} \right] & \text{2nd and 3rd neighbours} \end{cases}$$

where $\boldsymbol{r}$ is the distance vector, r^* is the position of the Lennard-Jones potential minimum, and κ and ε^* are the energy parameters.

The ground state of the lattice is characterized by the shear angle, a function of r^*/a, and the lattice parameter, a function of ε^*/κ. If $r^* \geqslant a$, the shear angle is non-zero. In that case, the second neighbours lie in the region where the second derivative of the Lennard-Jones

potential is negative, and the energy of a sheared square is lower than that of an unsheared one. We chose the shear angle to be 3° ($r^* = 1.2864483$, $a = 1$), in agreement with some representative real materials [13]. The energy parameters were adjusted accordingly. Domain structures and surface relaxation were then calculated by numerical minimization of the total energy functional:

$$\delta \int \mathrm{d}r^3 \left\{ \sum_{i,j} \mathcal{U}_p(i, j) \right\} = 0 \tag{2}$$

where $\mathcal{U}_p(i, j)$ is as defined in (1) and the sum extends over all lattice points.

A combination of two different boundary conditions was used in the simulation with free surface boundary conditions at the [010] and [$0\bar{1}0$] surfaces. The [100] and [$\bar{1}00$] edges of the simulated lattice were treated with derivative boundary conditions.

For elastic properties, the free surface boundary conditions might not seem appropriate, especially for non-large sizes of the simulated lattice, due to the long-range character of elastic forces. Since the essence of the problem addressed is the free surface, we were forced to use the free surface boundary conditions, and avoid problems by choosing a lattice large enough to avoid the surface–surface interaction, but within the scope of the available hardware on which the simulation has been run.

The derivative boundary conditions were the simplest to mimic the infinite extension of the simulated lattice in the given direction. This was crucial to allow the surface to relax freely, uninfluenced by any anomalies, with the exception of the domain wall simulated.

The present model has been studied by the molecular dynamics technique. We have not included any thermodynamic fluctuations, and have effectively simulated a system far from the ferroelastic–paraelastic transition temperature T_c. In order to study twin walls, without the influence of boundaries parallel to the walls and surface relaxation extending to $\sim$10% of the sample, a minimum of 80000 points were considered for a two-dimensional layer perpendicular to the surface and the twin wall.

Lattices simulated had initial conditions of no surface relaxation and infinitely narrow domain walls. We simulated a single wall in the middle of the lattice as well as an array of six walls distributed evenly throughout the simulated lattice, since in real materials microstructure usually forms a striped pattern, with domains of different orientations repeating periodically [14].

Since the simulation is only dealing with real space positions $X_{i,j}$ and $Y_{i,j}$ of each point (i, j) in the lattice, the output is a set of coordinates. This data was then manipulated to yield the $(xx - yy)$ component of the strain field throughout the simulated relaxed lattice.

The overall change in the lattice due to the relaxation effects is most easily observed in the distribution of the order parameter (proportional to the strain in the case of ferroelastics). Initially, the lattice was completely unrelaxed, with a domain wall between the twins of opposite orientations. The final strain distribution shows the consequences of the wall and surface relaxations (figure 1).

Far from the surface (in the bulk of the crystal) the wall relaxation follows the phenomenological Landau–Ginzburg model for the width of a twin domain wall [1, 15]:

$$\mathcal{Q}(x) = \mathcal{Q}_0 \tanh\left[\frac{x}{\mathcal{W}}\right]$$

where $\mathcal{Q}$ is the magnitude of the order parameter (strain), $\mathcal{Q}_0$ the value of the order parameter in the bulk, x the distance from the centre of the wall, and $\mathcal{W}$ the width of the domain wall. We have fitted the domain wall width $\mathcal{W}$ to our data and found it to be $\mathcal{W}$=10, measured in unit cells. This is in general agreement with the values for real materials

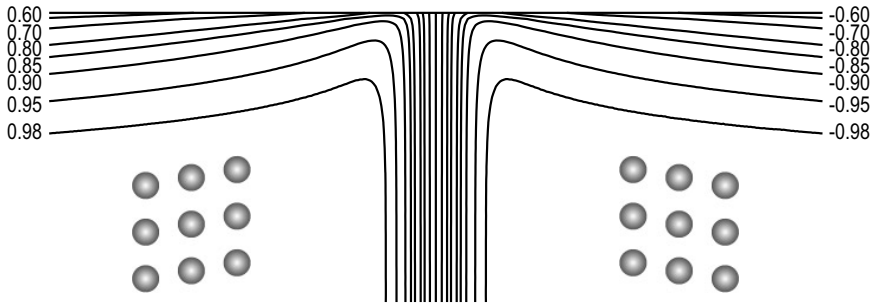

Figure 1. Distribution of the order parameter $\mathcal{Q}$ at the surface of the lattice (first 50 layers). Lines represent constant $\mathcal{Q}$, with $\mathcal{Q}_0 = 1$ in the bulk. There are three lines in the middle of the twin domain wall that are not labelled, they represent the $\mathcal{Q}$ values of 0.40, 0.00, and -0.40 respectively. Notice the steepness of the gradient of $\mathcal{Q}$ through the twin domain wall. The two structures represent sheared twin atomic configurations in the bulk (far from the twin domain wall and surfaces).

[13, 15, 16, 17]. Close to the surface the wall apparently widens in a characteristic trumpet-like shape, a consequence of both surface and domain wall origins of the relaxation effects. This can be seen from the widening of areas of constant strain. Still, the points of the maximum interaction between the surface and twin domain wall relaxation, where the lines of equal strain have the largest curvature, form a needle-like shape pointing towards the surface, a consequence of the surface relaxation being dominant at the surface and decreasing away from it. A calculation of the domain wall width at the surface, using the following expression:

$$\mathcal{Y}_s(x) = \mathcal{Y}_0 + \int_0^x \mathcal{Q}_s(t)\mathrm{d}t$$

where $\mathcal{Y}_s$ is the real space position of the particles in the surface layer, $\mathcal{Y}_0$ is the real space position of the particle at the centre of the domain wall, and $\mathcal{Q}_s$ is the distribution of the order parameter at the surface, has indicated that there is no appreciable difference between $\mathcal{W}$ and $\mathcal{W}_s$.

The surface relaxation depth λ is found to be at a minimum close to the twin domain wall and increasing with distance away from it. At an infinite distance λ would reach its maximum value λ_{max}, which is the surface relaxation depth of the lattice if no twin domain walls are present. Consequently, in materials with microstructure formed by an array of periodic twin domain walls, the depth of surface relaxation λ_{array} is suppressed, $\lambda_{array} < \lambda_{max}$. The order parameter at the surface $\mathcal{Q}_s$ exhibits exactly opposite behaviour.

The relation between $\mathcal{W}$ and $\mathcal{W}_s$, the domain wall widths in the bulk and at the surface, can most easily be seen if plotted on the same graph. The effect of the surface relaxation is clearly visible as the order parameter at the surface $\mathcal{Q}_s$ never reaches the bulk value $\mathcal{Q}_0$ (figure 2).

The distribution of the square of the order parameter $\mathcal{Q}_s^2$ at the surface shows the structure that some of the experimental works have been reporting [18, 19], namely a groove centred at the twin domain wall with two ridges, one on each side.

The real space topography of the surface is determined by both sources of relaxation—twin domain wall and the surface. These are distinct and when considered separately, we found the effect due to the wall relaxation larger by about three orders of magnitude than that due to the surface relaxation (figure 3).

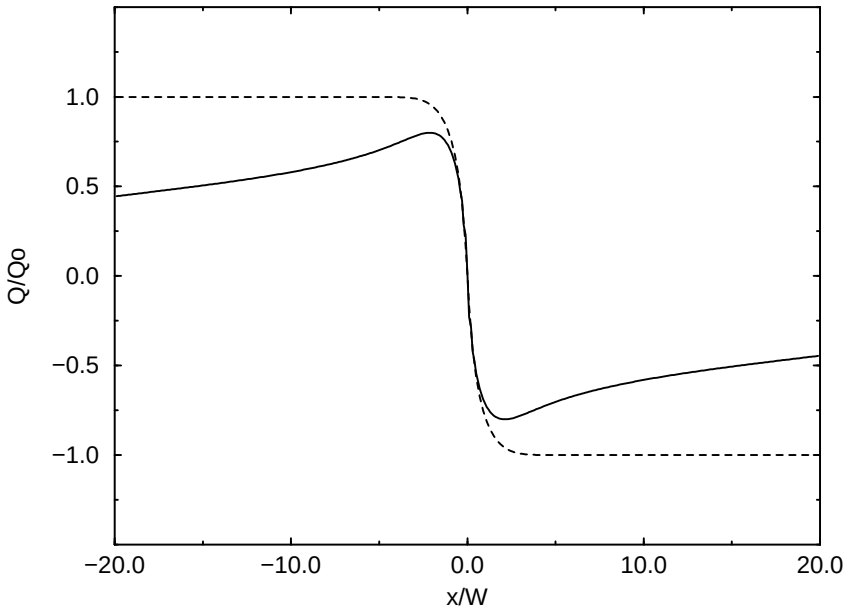

Figure 2. $\mathcal{Q}_s/\mathcal{Q}_0$ (solid line, proportional to the strain at the surface) and $\mathcal{Q}/\mathcal{Q}_0$ (dashed line, proportional to the strain in the bulk). The widths of the twin domain wall in the bulk, $\mathcal{W}$, and at the surface, $\mathcal{W}_s$, are the same, as is the width of the rounded at the surface directly above the twin domain wall.

The lattice features in the bulk are dominated exclusively by the domain wall relaxation, as the surfaces are too far away. This has provided us with a precise description of the relaxation due to the twin domain wall. By effectively removing this from the relaxed surface, we were left with the effects of the surface relaxation only. These yield a groove, centred at the twin domain wall, without any extra features. One recent analytical work [9] has in fact considered only the surface relaxation effects, while the much bigger wall relaxations were frozen, and a groove at the surface predicted, just as the one we obtained by removing the wall relaxation effects (figure 3). This result is incorrect, as it does not consider the problem completely. A groove only appears when the domain wall relaxation is ignored, yielding a wrong result, as the effects due to the wall relaxation are three orders of magnitude larger (displacements of particles due to the surface relaxation are $\sim 10^{-3}a$, whereas displacements due to the wall relaxation are $\sim a$, as can be seen in figure 3). In fact, the wall relaxation completely dominates the topography of the twin domain wall surface structure, entirely masking the groove-like effects originating in the surface relaxation, thus creating the surface rounding centred at the twin domain wall (figure 3). A recent AFM-tapping mode study [5] has identified this feature. It reports a 'nose' effect on the surface, that we have not been able to verify.

In an attempt to predict the possible experimental results of AFM investigations of the surface structure of the twin domain wall, we emulated the effect that the tip at the end of an AFM cantilever has on the surface of the material. This we did by displacing each particle in the surface layer by $10^{-8}a$ in the $-\hat{y}$ direction. We then calculated the lateral and normal components of the reactive force. The lateral force distribution shows a dependence similar to that of the order parameter $\mathcal{Q}_s$ (figure 4). The normal force distribution has a

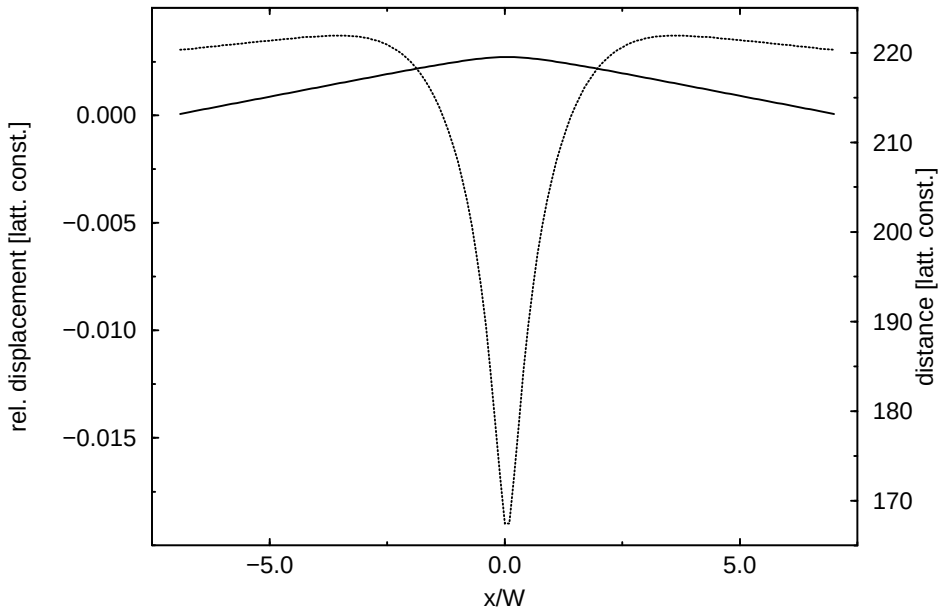

Figure 3. The surface topography (solid, right scale), and groove due to the wall relaxation (dotted, left scale), invisible in the topography of the surface. Notice the order of magnitude of surface deformation due to the domain wall.

profile similar to that of the square of the order parameter, $\mathcal{Q}_s^2$, with ridges on both sides of a groove (figure 4).

The change in the sign of the order parameter at the surface has been observed (for ferroelectrics) by using a mode of imaging developed for the detection of static surface charge [7]. For ferroelastics discussed here, this corresponds to the profile of the lateral reactive force. The SFM non-contact dynamic mode images [8] would correspond to the distribution of the normal reactive force. The divergence of the lateral force distribution away from the centre of the wall can be attributed to the simulated infinite extension of the lattice. In the simulated array, the lateral component of the force reached a finite value between two adjacent domain walls.

The results of this simulation can be used as a guidance for the future experimental work. In order to determine the twin domain wall width $\mathcal{W}$ in the bulk, one only needs to determine the characteristic width $\mathcal{W}_s$ of the surface structure of the domain wall. Previously, these features of the twinning materials were investigated using mainly x-ray techniques. We have shown that the only necessary ingredient for the determination of the twin domain wall width $\mathcal{W}$ are the real space positions of the particles in the surface layer.

In addition, we conclude that there are two levels of structure at the surface of the twin domain wall. The obvious structure, arising from the topography of the surface at the twin domain wall interface, is shown to be mainly featureless, apart from the rounding effects centred at the twin domain wall. We have shown that there is an underlying more interesting structure, its image obtainable via the elastic response of the particles in the surface layer. This structure consists of a groove centred at the surface of the twin domain wall and two ridges at the sides of the groove. Essentially it is a consequence of the strain distribution at the surface, itself a result of double relaxation originating from the surface and the twin

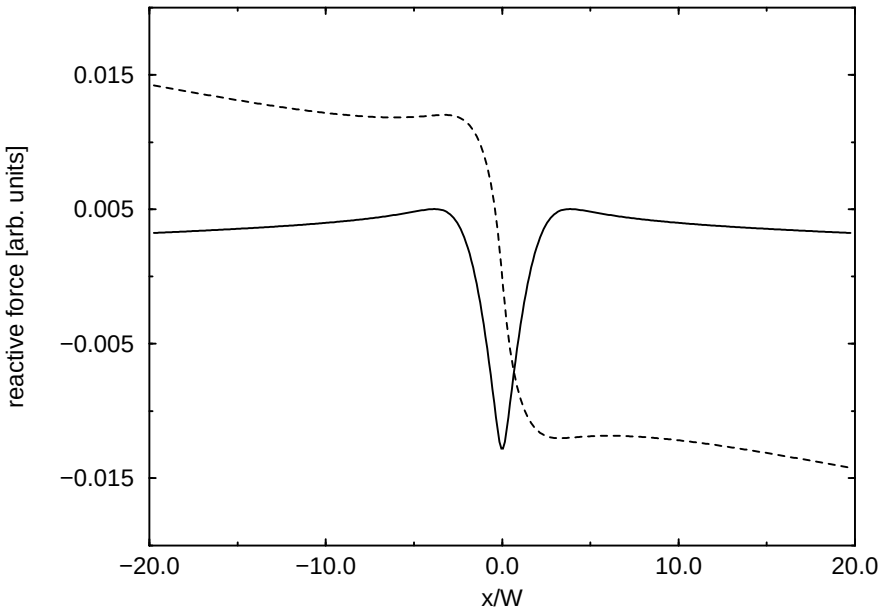

Figure 4. Distribution of the normal (solid line) and lateral (dashed line) response to normal displacement of the surface particles. Lateral response can be useful for observing the domain structure, while normal response can be useful for the observation of twin domain walls.

domain wall.

Finally, we comment on the chemical reactivity profile of the twin domain wall interface at the surface. Intuitively, one would expect the chemical reactivity of the surface to be the largest at the centre of the twin domain wall, falling off as the distance from the centre of the wall increases. In order to determine the chemical reactivity of the surface, one has to investigate the profile of the square of strain at the surface [20]. Contrary to the expected behaviour, chemically most reactive areas are at the sides of the twin domain wall, and the centre of the twin domain wall at the surface is the least reactive area. The reactivity does fall off as the distance from the centre of the wall increases, as expected, but only after it has reached a maximum at a distance of $\sim 3\mathcal{W}$.

If such a structure is exposed to particle adsorption (e.g. in the MBE growth of thin films on twinned substrates) we expect the sticking coefficient to vary spatially. In one scenario, adsorption may be enhanced on either side of the wall while being reduced at the centre.

The production runs of the simulation were carried out on the Hitachi S-3600/180 vector supercomputer, a part of the Cambridge High Performance Computing Facility.

References

[1] Salje E K H 1993 *Phase Transitions in Ferroelastic and Co-elastic Crystals* (Cambridge: Cambridge University Press)
[2] Mehta R V, Jagannathan R and Timmons J A 1996 *J. Imag. Sci. Technol.* **40** 77
[3] Amelinckx S, van Dyck D, van Landuyt J, van Tendeloo G 1997 *Handbook of Microscopy* (Weinheim: VCH)
[4] Chrosch J 1997 Private communication
[5] Bosbach D, Putnis A, Bismayer U and Güttler B 1997 *J. Phys.: Condens. Matter* **9** 8397

[6] Schönenberger C 1997 *Phys. World* **10**(9) 25
[7] Saurenbach F and Terris B D 1990 *Appl. Phys. Lett.* **56** 1703
[8] Lüthi R, Haefke H, Meyer K-P, Meyer E, Howald L and Güntherodt H-J 1993 *J. Appl. Phys.* **74** 7461
[9] Rychetský I 1997 *J. Phys.: Condens. Matter* **9** 4583
[10] Marais S, Heine V, Nex C and Salje E K H 1991 *Phys. Rev. Lett.* **66** 2480
[11] Bratkovsky A M, Marais S C, Heine V and Salje E K H 1994 *J. Phys.: Condens. Matter* **6** 3679
[12] Houchmanzadeh B, Lajzerowicz and Salje E K H 1992 *J. Phys.: Condens. Matter* **4** 9779
[13] Locherer K R, Hayward S A, Hirst P J, Chrosch J, Yeadon M, Abell J S and Salje E K H 1996 *Phil. Trans. R. Soc.* A **354** 2815
[14] Salje E K H and Parlinski K 1991 *Supercond. Sci. Technol.* **4** 93
[15] Wruck B, Salje E K H, Zhang M, Abraham T and Bismayer U 1994 *Phase Transitions* **48** 135
[16] Salje E K H 1995 *Phase Transitions* **55** 37
[17] Hayward S A, Chrosch J, Salje E K H and Carpenter M A 1996 *Eur. J. Mineral.* **8**
[18] Tsunekawa S, Hara K, Nishitani R, Kasuya A and Fukuda T 1995 *Mater. Trans., JIM* **36** 1188
[19] Tung Hsu and Cowley J M 1994 *Ultramicrosc.* **55** 302
[20] Houchmanzadeh B, Lajzerowicz J and Salje E K H 1991 *J. Phys.: Condens. Matter* **3** 5163